

# Characterization of the Acid–Base Properties of the TiO<sub>2</sub>(110) Surface by Adsorption of Amines

Enrique Farfan-Arribas and Robert J. Madix\*

Chemical Engineering Department, Stanford University, Stanford, California 94305-5025

Received: October 31, 2002; In Final Form: February 7, 2003

The adsorption of ammonia, dimethylamine, and ethylamine on stoichiometric and slightly defective TiO<sub>2</sub>-(110) surfaces was studied by means of TPRS and XPS. The slightly defective surfaces were prepared by exposing a clean stoichiometric surface to electron irradiation, resulting in the creation of point defects (oxygen vacancies) while minimizing the structural damage inflicted to the surface. Adsorption is proposed to take place on this surface by the binding of the nitrogen atom in the amine to a Ti<sup>4+</sup> cation. On the stoichiometric surface, the amines adsorbed and desorbed primarily intact, with a small fraction (5–8%) nonselectively decomposing into CO, N<sub>2</sub>, and H<sub>2</sub> in the cases of dimethylamine and ethylamine. On the defective surfaces, the adsorption behavior of the amines was not significantly altered, as they still adsorbed and desorbed mainly intact. The observed coverage on the defective surfaces was smaller (3–19%) than that on the stoichiometric surface, suggesting that adsorption on the point defects blocks adsorption at more than one neighboring Ti<sup>4+</sup> cation. The activation energies for desorption of the amines on the TiO<sub>2</sub>(110) surface were shown to correlate with the gas-phase basicities of these species, reflecting the Lewis acid character of the Ti<sup>4+</sup> cations.

## Introduction

The adsorption of ammonia on TiO<sub>2</sub> rutile powders and single crystals has been extensively studied.<sup>1–6</sup> Diebold and Madey used LEIS and XPS to show that NH<sub>3</sub> chemisorbed molecularly on TiO<sub>2</sub>(110) and desorbed completely below 395 K.<sup>3</sup> UPS experiments by Román et al.<sup>2</sup> also showed that NH<sub>3</sub> adsorbed intact and desorbed below 370 K. Epling et al.<sup>6</sup> compared the desorption spectra of NH<sub>3</sub> on TiO<sub>2</sub>(110) surfaces that had been subjected to different oxidation treatments and found that desorption occurred molecularly in two states, with the temperature and population of each depending on the oxidation treatment. One of the objectives of this work is to characterize the desorption spectrum of NH<sub>3</sub> for a series of different coverages to further the understanding of the NH<sub>3</sub>/TiO<sub>2</sub>(110) system.

TiO<sub>2</sub> is considered to be an ideal material for the study of surface defects.<sup>7–9</sup> Three techniques have been used to produce relatively reproducible populations of defects on TiO<sub>2</sub>(110): (1) Ar<sup>+</sup> bombardment, (2) annealing in UHV, and (3) electron irradiation. All of these treatments result in the creation of oxygen vacancies, producing Ti<sup>3+</sup> cations and effectively reducing the surface. Ar<sup>+</sup> bombardment acts by preferentially sputtering oxygen from the surface and produces a wide variety of reduced Ti states (Ti<sup>3+</sup>, Ti<sup>2+</sup>).<sup>8,10</sup> Annealing in UHV to moderate temperatures (<1200 K) results in the appearance of Ti<sup>3+</sup> in XPS, due to point defects created by the entropy-driven preferred desorption of oxygen.<sup>11</sup> Annealing at higher temperatures (>1200 K) results in the formation of a (1 × 2) reconstructed surface, as evidenced by LEED and STM.<sup>12,13</sup> Electron irradiation at moderate energies causes little damage to the surface and produces Ti<sup>3+</sup> exclusively.<sup>14,15</sup> The advantage of using electron irradiation for defect creation purposes is that different populations of defects on the surface can be obtained by varying the time of exposure to the beam.

The study of defects by adsorbing probe molecules has contributed to the understanding of the active sites on TiO<sub>2</sub>-(110). Small molecular probes such as CO, N<sub>2</sub>O, H<sub>2</sub>O, HCOOH, O<sub>2</sub>, and H<sub>2</sub> have been used on TiO<sub>2</sub> single-crystal surfaces in an attempt to understand the reactivity of these defect sites.<sup>11,15–19</sup> Defects were found to alter the characteristics of the adsorption of some of these molecules, promoting dissociative over molecular adsorption. Several of these adsorbates might also be involved in redox reactions with the surface, in which the reduced Ti<sup>3+</sup> is oxidized by the adsorbates to Ti<sup>4+</sup>.

The adsorption of ammonia on defective TiO<sub>2</sub>(110) surfaces has also been subject to study. So far, previous work has concentrated on vacuum-annealed (slightly defective) and Ar<sup>+</sup>-sputtered (highly defective) surfaces. NH<sub>3</sub> appears to adsorb molecularly on these surfaces as well. Whereas Diebold and Madey<sup>3</sup> saw no evidence of thermally induced dissociation, Román et al.<sup>2</sup> suggested that a small fraction of the adsorbed ammonia might have decomposed when heated over 300 K. The issue of whether defects affect the saturation coverage of NH<sub>3</sub> on the surface is also unclear. The first study showed almost no variation in coverage within experimental error, whereas the second predicted a decrease of ~20% from the stoichiometric surface. In an APECS study, Siu et al.<sup>1</sup> estimated that only a small reduction of the saturation coverage should be expected on this surface. In this work, we address these issues further by analyzing the desorption spectra of ammonia from surfaces with different defect populations created by electron bombardment.

Acid–base catalysis is of great importance in many industrial applications, such as catalytic cracking, isomerization, alkylation, acylation, polymerization, hydrolysis, dehydrogenation, and esterification reactions. A detailed understanding of these reactions at the molecular level requires knowledge of the acid–base properties of these catalysts. Several methods for determining the acid–base properties of solid surfaces have been discussed previously in the literature.<sup>20–22</sup> Among these methods

\* Corresponding author. E-mail: rjm@chemeng.stanford.edu.

are IR spectroscopy, temperature-programmed desorption, liquid-phase titration, pH at zero net surface charge measurements, contact angle measurements, microcalorimetry, X-ray photoelectron spectroscopy, and inverse gas chromatography. These techniques require the adsorption of molecules of known acid or basic properties so that the acid–base behavior of the surface can be related to those of the probe molecules.

Several such relationships have been obtained for the dissociation of Brønsted acids on metal and oxide surfaces. For example, titration/displacement experiments on Ag(110) have shown that the relative Brønsted acidities of adsorbed species correlate with the gas-phase acidity scale of the probe molecules.<sup>23</sup> In the case of oxides, titration/displacement studies on ZnO and MgO powders established that the relative acidity scales of these oxides were in better agreement with the aqueous dissociation constants than with the gas-phase acidity scale of the adsorbed molecules, suggesting that the surfaces acted as solvents in providing stabilization of the charge on the conjugate base anion.<sup>24</sup> Temperature-programmed desorption of basic molecules such as ammonia and pyridine has been frequently used to evaluate the acid strength and acid amount on solid surfaces.<sup>21</sup> The desorption temperature of the molecule from the surface is a direct measure of the strength of the acidic site, and the area under the TPD peak is proportional to the amount adsorbed. In this paper, we use this method to evaluate the Lewis acidity of the TiO<sub>2</sub>(110) surface by adsorbing three basic probe molecules: ammonia, dimethylamine, and ethylamine. Although pyridine is usually preferred for this type of study, previous work on the pyridine/TiO<sub>2</sub>(110) system concluded that pyridine does not form stable N–Ti bonds with the Ti<sup>4+</sup> sites, but rather adsorbs weakly with the aromatic ring parallel to the surface<sup>25–27</sup> and thus does not represent an accurate measure of the acidity of the Ti<sup>4+</sup> cations.

## Experimental Section

The experiments were conducted in a two-chamber ultra-high-vacuum (UHV) apparatus that has been described in detail elsewhere.<sup>28</sup> Base pressures in the preparation and analysis chambers were  $\sim 6 \times 10^{-10}$  and  $\sim 2 \times 10^{-10}$  Torr respectively. The preparation chamber is equipped with variable leak valve dosers and a sputtering gun (Physical Electronics) and is used mainly for sample cleaning procedures. The analysis chamber is equipped with LEED optics, a Perkin-Elmer 04-548 dual-anode X-ray source, a SPECS EA-10 Plus hemispherical energy analyzer, a UTIc100 quadrupole mass spectrometer (QMS), and a needle gas doser.

Temperature-programmed reaction spectroscopy (TPRS) experiments were performed using the computer-controlled QMS in two different scan modes. First, complete product identification was achieved by monitoring 100 masses simultaneously at low resolution. Subsequently, high-resolution spectra were obtained by monitoring only 16 masses at a time. The ionizer of the mass spectrometer was enclosed in a glass cap with a small hole at the end facing the surface to be studied, to ensure that only those species desorbing from the crystal contributed to the TPRS spectrum. Quantification of each product was achieved using its most intense mass fragment, after accounting for sensitivity factors and contributions of other products to that mass. The fragmentation patterns used for product identification were obtained by leaking the samples into the background of the analysis chamber. During the TPRS and XPS measurements, the analysis chamber was isolated from the preparation chamber.

The rutile TiO<sub>2</sub>(110) single crystal ( $10 \times 10 \times 1$  mm<sup>3</sup>, Atomergic Chemetals Corp.) was mounted on a tantalum support

using a ceramic adhesive (Ceramabond, Aremco Products) to ensure good contact. The crystal temperature was measured by a chromel–alumel thermocouple glued into a hole on the side of the crystal with the aforementioned adhesive. Sample temperatures of up to 900 K were achieved by resistively heating the tantalum foil via two tantalum wires. Prior to use, the crystal was rendered conductive by an extended high-temperature annealing in UHV, to prevent charging problems during XPS measurements. The crystal changed color to light blue as this process created an oxygen-deficient bulk. The crystal was cleaned daily in the preparation chamber by two 15-min Ar<sup>+</sup> sputtering cycles (500 eV,  $5 \times 10^{-5}$  Torr) followed by a 15-min anneal in oxygen ( $10^{-6}$  Torr) to 850 K and then cooled to room temperature in the same oxygen atmosphere. This procedure resulted in a well-ordered, clean surface as evidenced by a sharp ( $1 \times 1$ ) LEED pattern and XPS spectrum. This surface was stoichiometric as revealed by the absence of a shoulder on the Ti(2p) XPS spectrum, indicating that no Ti<sup>3+</sup> ions were present within the limits of detection of this technique. It is likely that, because of the oxygen anneal, a small population of adsorbed oxygen was present on the surface even though it was not observed in the O(1s) XPS peak.

Defects on this surface were created by electron-beam irradiation, which has been shown to produce anion point defects by electron-stimulated desorption (ESD) of surface bridging oxygen ions.<sup>14,29</sup> Electron bombardment was achieved by biasing the crystal surface at 300 V and exposing it to electrons emitted from a nearby hot filament. This choice of electron energy was high enough that it allowed the creation of detectable populations of defects using short exposure times, but low enough that it did not result in significant structural damage to the surface, as discussed in the Surface Characterization section. The current measured through the crystal was  $\sim 1$  mA, but because the entire sample holder was exposed to the electron beam, the actual current on the sample was significantly lower.

Ammonia (99% anhydrous, Aldrich), dimethylamine (99%, Aldrich), and ethylamine (97% anhydrous, Aldrich) were used as supplied by the manufacturer. The purities of the samples were checked by leaking each reactant into the analysis chamber while measuring its cracking pattern with the mass spectrometer. In all experiments, the reactants were dosed to saturation coverage at room temperature by means of variable leak valves. The heating rate in the TPRS and in the temperature series for the XPS experiments was 3 K/s.

## Results and Discussion

**Surface Characterization.** The TiO<sub>2</sub>(110) surface was characterized by means of XPS before each experiment. After the cleaning procedure, only one Ti(2p<sub>3/2</sub>) peak was observed in the XPS spectrum. This Ti(2p<sub>3/2</sub>) XPS peak was symmetric and exhibited a binding energy of 459.2 eV, characteristic of Ti<sup>4+</sup>(2p<sub>3/2</sub>) on rutile (110) surfaces.<sup>30,31</sup> The surface prepared in this fashion was stoichiometric, and it is referred to as a “defect-free” surface.

Electron bombardment was chosen over Ar<sup>+</sup> sputtering for defect creation because this technique does not significantly damage the overall surface structure.<sup>13,14</sup> LEED patterns for electron-bombarded TiO<sub>2</sub>(110) surfaces at 300 eV have shown that the ( $1 \times 1$ ) structure is clearly discernible up to beam exposure times of 15 min, whereas a 1-min exposure to Ar<sup>+</sup> completely destroys the long-range order of the surface.<sup>28</sup> Recently, our own STM studies have shown that images of vacuum-annealed TiO<sub>2</sub>(110) surfaces are very similar to images of electron-bombarded surfaces and, in both cases, the long-range order of the surface is preserved.<sup>32</sup>

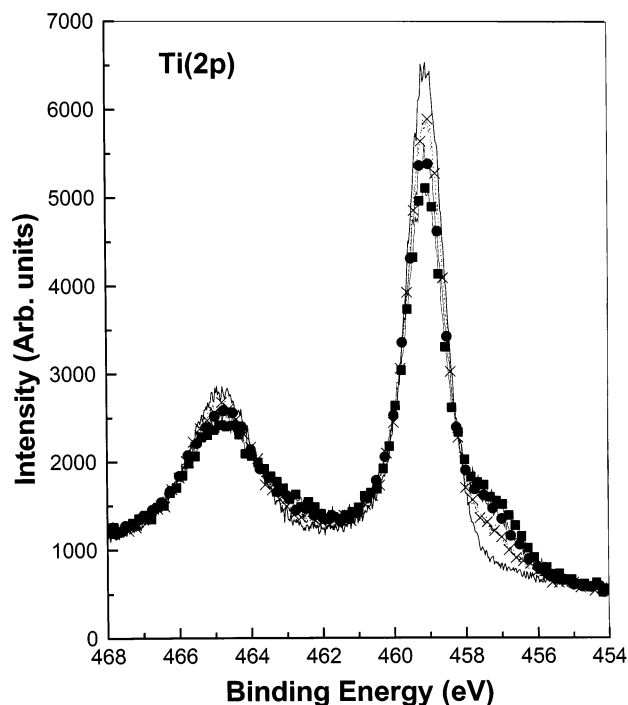


**Figure 1.** Ti(2p) XPS spectra for the TiO<sub>2</sub>(110) surface as a function of electron beam exposure time. (—) No exposure to electrons, (x) 3-min exposure, (●) 5-min exposure, (■) 10-min exposure.

**TABLE 1. Total Ti<sup>3+</sup> and Ti<sup>4+</sup> Concentrations as a Function of Surface Exposure Time to Electron Beam and Ar<sup>+</sup> Sputtering**

	electron bombardment time (min)					Ar <sup>+</sup> (min)
	0	1	3	5	10	0.5
Ti <sup>4+</sup> concentration (%)	100	97.5	95.2	91.0	88.0	87.0
Ti <sup>3+</sup> concentration (%)	0	2.5	4.8	9.0	12.0	13.0

After electron irradiation at 300 eV, the presence of defects was confirmed by the appearance of a second XPS peak in the form of a shoulder on the lower-binding-energy side of the Ti<sup>4+</sup>(2p<sub>3/2</sub>) peak, which indicated the presence of lower-valence Ti cations. Figure 1 shows the XPS spectra for the Ti(2p) level for different electron beam exposures. The low-energy shoulder was found to increase in magnitude with electron exposure, as expected. Upon deconvolution, the binding energy of this second Ti(2p<sub>3/2</sub>) peak is found to be 457.4 eV. This binding energy value suggests that only Ti<sup>3+</sup> defects were produced by this method, as it has been observed previously observed that the Ti<sup>3+</sup>(2p<sub>3/2</sub>) peak has a binding energy  $\sim 1.8$  eV lower than that of Ti<sup>4+</sup>(2p<sub>3/2</sub>).<sup>8,10</sup>

The different concentrations of defects produced by varying the exposure time of the surface to the electron beam are reported in Table 1. A surface exposed to Ar<sup>+</sup> bombardment for 30 s is also shown for comparison. The concentration of Ti<sup>3+</sup> cations varied from 0 to 12% with increasing electron beam exposure. For the largest exposure at 10 min, the concentration of defects produced was similar in magnitude to that produced by Ar<sup>+</sup> bombardment for 30 s.

**Ammonia.** The desorption spectra obtained for different exposures of NH<sub>3</sub> at room temperature onto the clean stoichiometric TiO<sub>2</sub> surface are shown in Figure 2. For each exposure, NH<sub>3</sub> was the only product that desorbed from the surface. Other possible decomposition products such as nitrogen and nitrogen oxides were monitored as well but were not present. NH<sub>3</sub> was found to desorb at approximately 335 K independent of

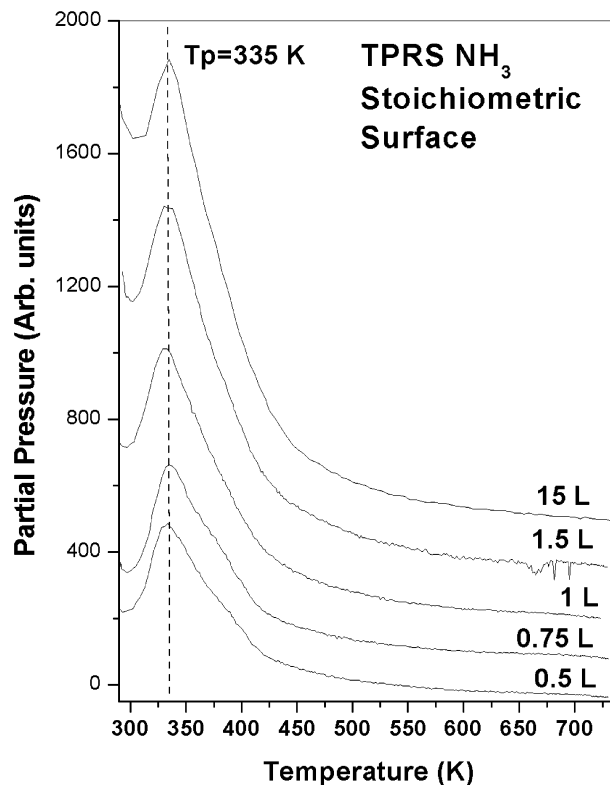


**Figure 2.** Desorption spectra obtained for different exposures of NH<sub>3</sub> at room temperature onto the stoichiometric TiO<sub>2</sub>(110) surface. NH<sub>3</sub> desorption is represented by a mass-to-charge ratio of 17.

coverage. Epling et al.<sup>6</sup> have reported ammonia TPD spectra for different surface preparation conditions. The ammonia peak they obtained from the vacuum-annealed surface was broad and exhibited a high-temperature shoulder, similar to the peaks we obtained at low coverage (0.5–0.75 L) on our stoichiometric surface. This feature became larger and shifted to higher temperature as the surface was oxidized and was attributed to a more strongly bound state of ammonia due to adsorption on oxygen adatoms. This behavior was not observed in our oxidized surface at higher ammonia doses (1–15 L), suggesting that oxygen adatoms were not present, or if they were, they were not playing a significant role in the adsorption of ammonia in this case.

A series of nitrogen 1s XPS spectra for a saturation exposure of NH<sub>3</sub> at room temperature onto the clean, stoichiometric TiO<sub>2</sub> surface are shown in Figure 3. After adsorption at room temperature (curve a), the only N(1s) peak observed was centered at a binding energy of 400.1 eV with a full width at half-maximum (fwhm) of 1.02 eV. This peak was assigned to molecularly adsorbed NH<sub>3</sub>, because the binding energy value is in good agreement with previously reported values for this species.<sup>3</sup> After the surface had been flashed to 400 K and cooled back to room temperature (curve b), the N(1s) peak disappeared almost in its entirety. Heating the surface past 400 K returned the signal to background levels, indicating that no nitrogen-containing compounds were left on the surface.

The adsorption behavior of NH<sub>3</sub> onto surfaces with different populations of point defects was not significantly different from the behavior on the stoichiometric surface. The desorption spectra obtained for a saturation coverage of NH<sub>3</sub> on TiO<sub>2</sub>(110) surfaces that had been previously irradiated with electrons are shown in Figure 4. As in the case of the stoichiometric surface, only NH<sub>3</sub> was found to desorb from these surfaces. NH<sub>3</sub> desorption from these surfaces occurred at slightly lower

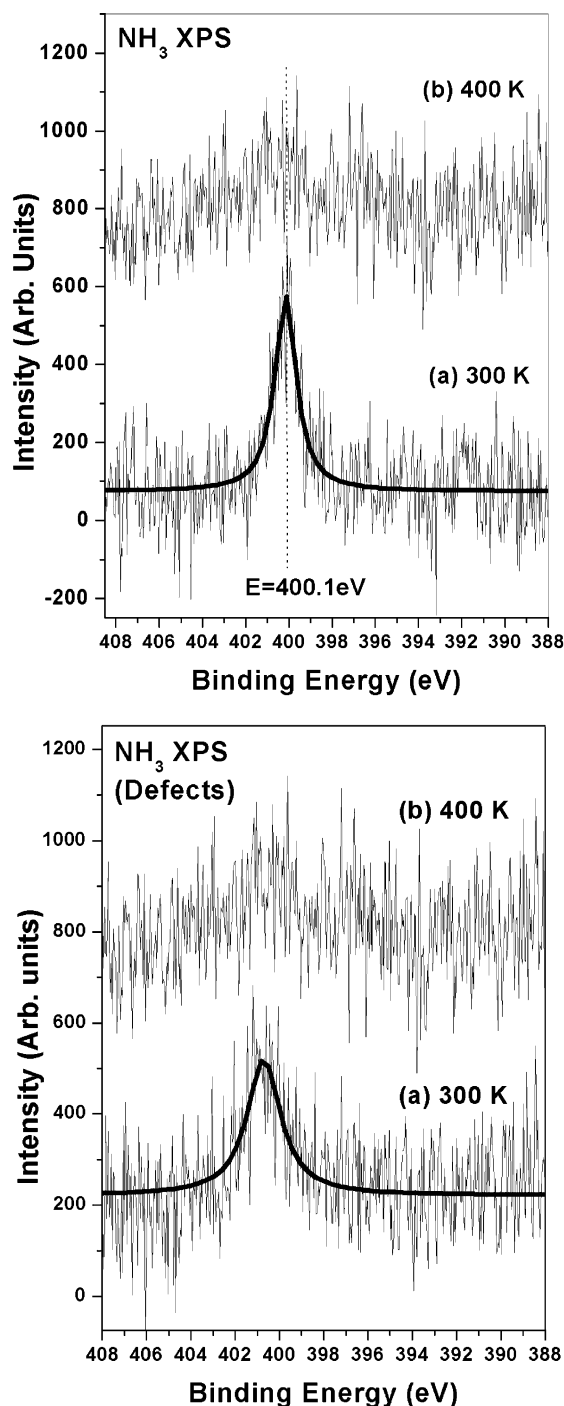


**Figure 3.** Nitrogen 1s XPS spectra after a saturation exposure of  $\text{NH}_3$  onto the stoichiometric (top) and 3-min electron-irradiated (bottom)  $\text{TiO}_2(110)$  surfaces taken at room temperature. (a) Surface after  $\text{NH}_3$  exposure at room temperature, (b) surface in a after being flashed to 400 K.

temperatures (327 K, 332 K) than desorption from the stoichiometric surface (335 K). The N(1s) XPS series of spectra obtained after  $\text{NH}_3$  adsorption at room temperature on the defective surface (3-min exposure) is shown in Figure 3. As in the case of the stoichiometric surface, after adsorption at 300 K (curve a) only one nitrogen peak was detected, and it had a binding energy of 400.6 eV and a fwhm of 1.7 eV. Heating the surface to 400 K (curve b) resulted in the disappearance of this feature, indicating that no nitrogen was left on the surface.

Integration of the areas under the TPD desorption curves revealed that the coverage on the defective surfaces decreased

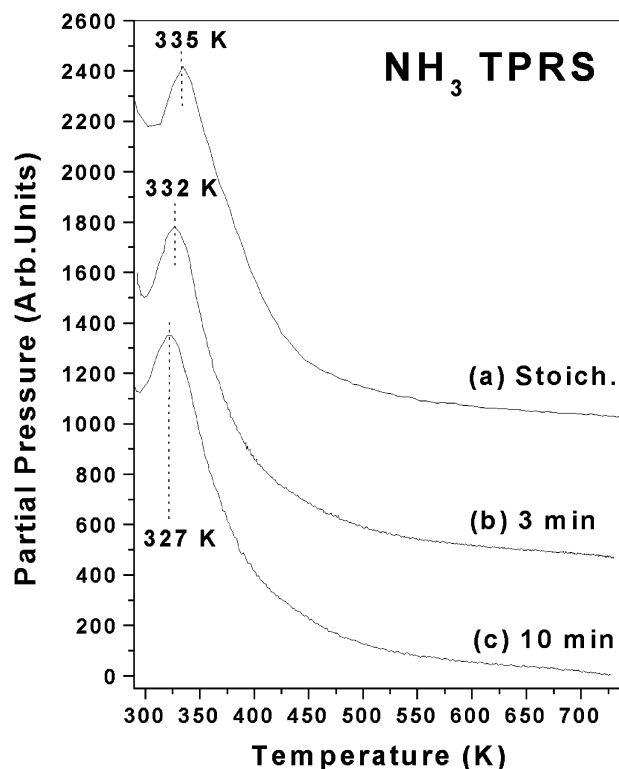


**Figure 4.** Desorption spectra obtained for a saturation coverage of  $\text{NH}_3$  on  $\text{TiO}_2(110)$  surfaces that had been previously irradiated with electrons. (a) Stoichiometric surface shown for comparison, (b) surface preexposed to 300 eV electrons for 3 min, (c) surface preexposed to 300 eV electrons for 10 min.

with respect to that on the stoichiometric surface by  $\sim 19$  and  $\sim 11\%$  on the 3- and 10-min electron-irradiated surfaces, respectively. The fact that the reduction in coverage is smaller for the 10-min irradiated surface can be attributed to the possible existence of local reconstructions in cases of large oxygen deficiencies, as when the surface is subjected to long electron irradiation times. Similar behavior has been observed in the case of alcohols adsorbed on electron-irradiated  $\text{TiO}_2(110)$  surfaces, where the maximum amount of products was obtained not at the highest electron exposures, but at an intermediate exposure.<sup>33</sup> A comparison of the areas under the N(1s) XPS peaks indicates a reduction in coverage on the 3-min exposed surface of  $\sim 25\%$  compared to that of the stoichiometric surface, in reasonably good agreement with the TPD measurements. The existing evidence in the literature on whether defects influence  $\text{NH}_3$  coverage on  $\text{TiO}_2(110)$  is not conclusive. Román et al.<sup>2</sup> determined by means of UPS that the coverage was 20–30% lower on a vacuum-annealed surface than on the stoichiometric surface. Diebold and Madey<sup>3</sup> calculated the  $\text{NH}_3$  coverages by means of XPS for stoichiometric, slightly oxygen-deficient (vacuum-annealed) and highly oxygen-deficient (Ar-sputtered) surfaces and found them to be roughly equal ( $\pm 20\%$  error). Siu et al.<sup>1</sup> estimated a small reduction of the saturation coverage on the vacuum-annealed surface based on their Auger-photoelectron coincidence spectroscopy (APECS) measurements. Our results support the claims that coverage is, in fact, reduced when point defects are present on the  $\text{TiO}_2(110)$  surface.

The results obtained in this paper support the model for  $\text{NH}_3$  adsorption proposed by Diebold and Madey<sup>3</sup> and later refined by Siu et al.<sup>1</sup> In this model,  $\text{NH}_3$  is proposed to adsorb molecularly with the N end down on every other  $\text{Ti}^{4+}$  cation on the stoichiometric surface. On the defective surface,  $\text{NH}_3$  is proposed to adsorb on the bridging oxygen vacancies as well.



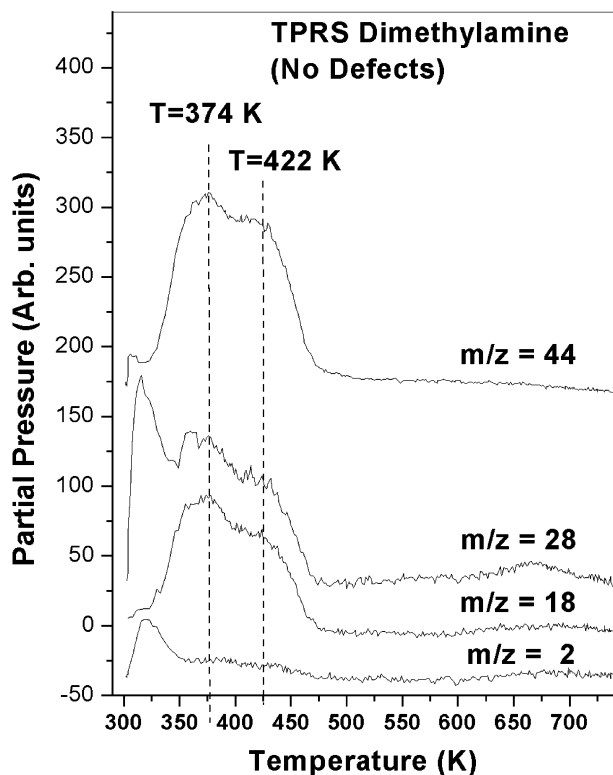


**Figure 5.** Desorption spectrum obtained after a saturation dose of dimethylamine at room temperature onto the stoichiometric  $\text{TiO}_2(110)$  surface.

Given a van der Waals diameter of 3.6 Å for  $\text{NH}_3$ , an ammonia molecule adsorbed on an oxygen vacancy site will block one or two adjacent  $\text{Ti}^{4+}$  sites, effectively reducing the coverage. It is important to note that this model was developed using coverage arguments and that there is no evidence that  $\text{NH}_3$  actually forms an ordered overlayer. STM studies should be helpful in ascertaining whether this is the case.

Regardless of the actual arrangement of  $\text{NH}_3$  on the surface, the fact that  $\text{NH}_3$  is coordinated via the electron lone pair to the Lewis-acidic surface  $\text{Ti}^{4+}$  cations<sup>5</sup> provides an opportunity to investigate the relative Lewis acidity of these cations by comparison with other amines of different basicities. Traditionally, pyridine has been chosen for this purpose. However, previous work on the pyridine/ $\text{TiO}_2(110)$  system concluded that pyridine does not form stable N–Ti bonds with the  $\text{Ti}^{4+}$  sites, but rather adsorbs weakly with the aromatic ring parallel to the surface.<sup>25–27</sup> We chose dimethylamine and ethylamine for our acid/base study because they are expected to bond through the N lone pair to the  $\text{Ti}^{4+}$  and span an appropriate range of Lewis basicities.

**Dimethylamine.** The desorption spectrum obtained after a saturation dose of dimethylamine is shown in Figure 5. Dimethylamine desorbed intact in two states at 374 and 422 K, as evidenced by the simultaneous evolution of mass fragments 44, 28, and 18. The two desorption states were too close in temperature to be completely resolved. In addition, a small fraction ( $\sim 5\%$ ) of dimethylamine decomposition products evolved as CO,  $\text{N}_2$ , and  $\text{H}_2$  at  $\sim 315$  K.

The N(1s) XPS spectrum obtained after a saturation dose of dimethylamine on the stoichiometric  $\text{TiO}_2(110)$  surface at room temperature is shown in Figure 6. The spectrum taken after adsorption (curve a) shows only one nitrogen peak, centered at 401.1 eV with a fwhm of 1.4 eV. The observed binding energy was similar to that of nitrogen in  $\text{NH}_3$ , and therefore, this peak

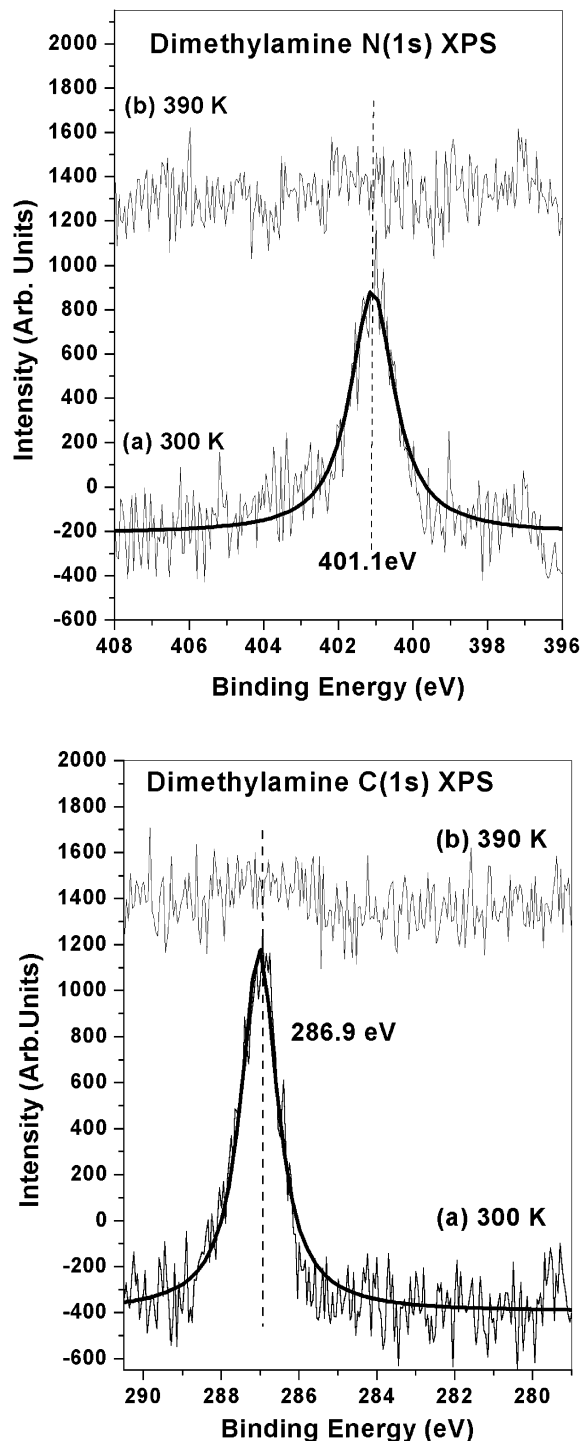


**Figure 6.** Nitrogen 1s XPS spectra (top) and carbon 1s XPS spectra (bottom) obtained after a saturation exposure of dimethylamine onto the stoichiometric  $\text{TiO}_2(110)$  surfaces taken at room temperature. (a) Surface after dimethylamine exposure at room temperature, (b) surface in a after being flashed to 390 K.

was assigned to the nitrogen in dimethylamine. The similarity in binding energies suggests that dimethylamine is also bound to the  $\text{Ti}^{4+}$  cations through the nitrogen atom. If the second dimethylamine TPD desorption state corresponded to dimethylamine bound at a different binding site, such as an oxygen adatom, we would most likely have observed a second XPS peak at a different binding energy. However, this is not an entirely conclusive result because it is possible that dimethylamine could bind to an oxygen adatom without substantially changing the binding energy of its nitrogen atom with respect

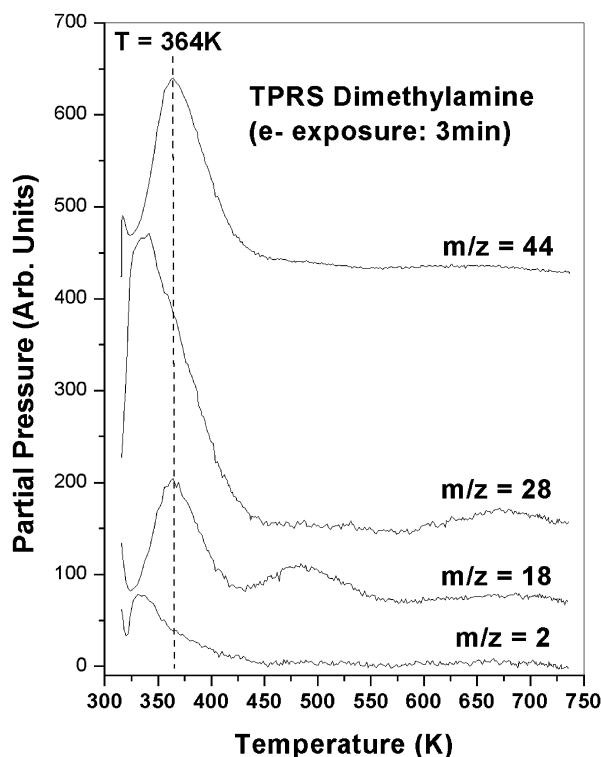


**Figure 7.** Desorption spectrum obtained after dimethylamine adsorption at room temperature on the defective (3-min exposure)  $\text{TiO}_2(110)$  surface.

to the adsorbate at the  $\text{Ti}^{4+}$  site. In an attempt to distinguish between these two desorption states observed in TPD, the surface was heated to 390 K and cooled back to room temperature. The  $\text{N}(1s)$  signal was shown to decrease to background levels (curve b), and no clear peaks were observed.

The  $\text{C}(1s)$  XPS spectrum obtained after a saturation dose of dimethylamine on the stoichiometric  $\text{TiO}_2(110)$  surface at room temperature is shown in Figure 6. Upon adsorption (curve a), the spectrum showed only one peak centered at 286.9 eV with a fwhm of 1.14 eV. The fact that only one carbon environment was observed supports the claim that dimethylamine is adsorbed intact on this surface. The binding energy observed is in excellent agreement with those reported for carbon bound to oxygen in aliphatic alcohols adsorbed on this surface.<sup>33</sup> The similarity in binding energies and structure between these alcohols and dimethylamine leads us to suggest similar binding arrangements in the two cases. Because the alcohols are bound through the oxygen atom to the  $\text{Ti}^{4+}$  cations, dimethylamine is proposed to bind through the nitrogen atom to these cations. After the surface to 390 K had been heated and cooled back to room temperature (curve b), the  $\text{C}(1s)$  signal returned to background levels, suggesting that no carbon-containing compounds were left on the surface.

The influence of point defects on dimethylamine adsorption on  $\text{TiO}_2(110)$  was studied on a surface that had been preexposed to electron irradiation for a period of 3 min. The TPD spectrum after adsorption of dimethylamine at room temperature on such a surface is shown in Figure 7. The first significant difference in the spectrum is that there is only one desorption state observed for dimethylamine ( $m/z = 44$ ), as opposed to the two on the stoichiometric surface. This result seems to support the idea that the high-temperature dimethylamine desorption feature observed on the stoichiometric surface corresponds to dimethylamine bound to an oxygen adatom, because exposing the surface to 300 eV electrons would have removed the existing oxygen

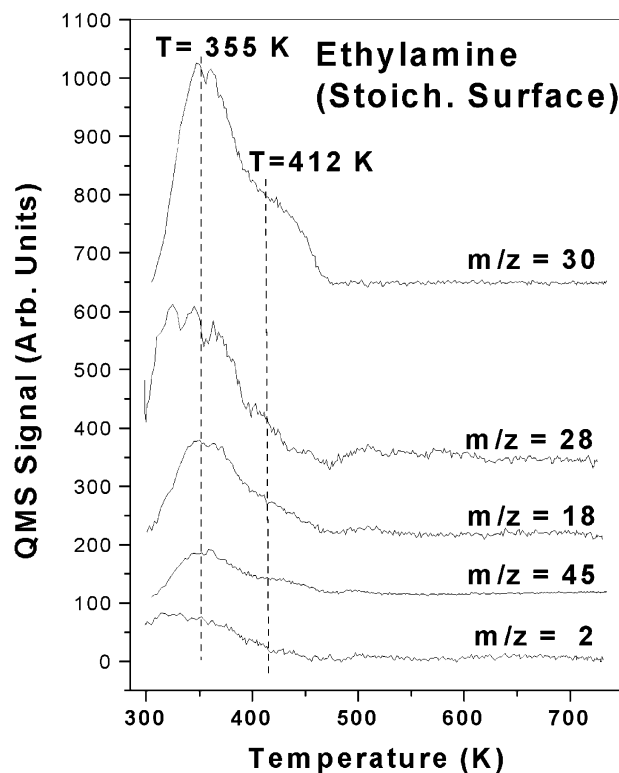


**Figure 8.** Desorption spectrum obtained after a saturation dose of ethylamine on the stoichiometric  $\text{TiO}_2(110)$  surface at room temperature.

adatoms,<sup>34</sup> so that the second peak would no longer be present on the defective surface. The only dimethylamine peak evolved at 364 K, which represents a 10 K shift to lower temperature. Peak shifts to lower temperatures of similar magnitude have been previously observed in the presence of defects for alcohols adsorbed on  $\text{TiO}_2(110)$ .<sup>33,35</sup> Decomposition products from dimethylamine such as  $\text{CO}$ ,  $\text{N}_2$ , and  $\text{H}_2$  were also observed on the defective surface, but their proportions did not vary significantly from those on the stoichiometric surface. This behavior does not parallel that of the alcohols, where decomposition products were shown to increase markedly with increased defect population, suggesting that adsorption on the defects is not responsible for the decomposition products in the case of dimethylamine. Water desorption from the surface is also observed at  $\sim 485$  K and attributed to adsorption of water from the background on the point defects. Henderson has shown that recombination of OH from oxygen vacancies created by electron bombardment occurs between 300 and 500 K, depending on electron energy.<sup>36</sup> Integration of the areas under the TPD curves revealed that the coverage of dimethylamine on the defective surface was 7% lower than that on the stoichiometric surface. Similarly to ammonia, this would seem to indicate that adsorption on defects blocks access to the  $\text{Ti}^{4+}$  sites, resulting in an overall decrease in coverage.

**Ethylamine.** The desorption spectrum obtained after a saturation dose of ethylamine at room temperature on the stoichiometric  $\text{TiO}_2(110)$  surface is shown in Figure 8. As in the case of dimethylamine, ethylamine desorbed intact in two different states evolving at 355 and 412 K, as indicated by mass-to-charge ratios 45, 30 and 28. A small fraction ( $\sim 8\%$ ) of decomposition products such as  $\text{CO}$ ,  $\text{N}_2$ , and  $\text{H}_2$  was observed at  $\sim 330$  K.

The  $\text{N}(1s)$  XPS spectrum obtained after ethylamine adsorption at room temperature on the stoichiometric  $\text{TiO}_2(110)$  surface is shown in Figure 9. The only nitrogen peak was centered at 400.6

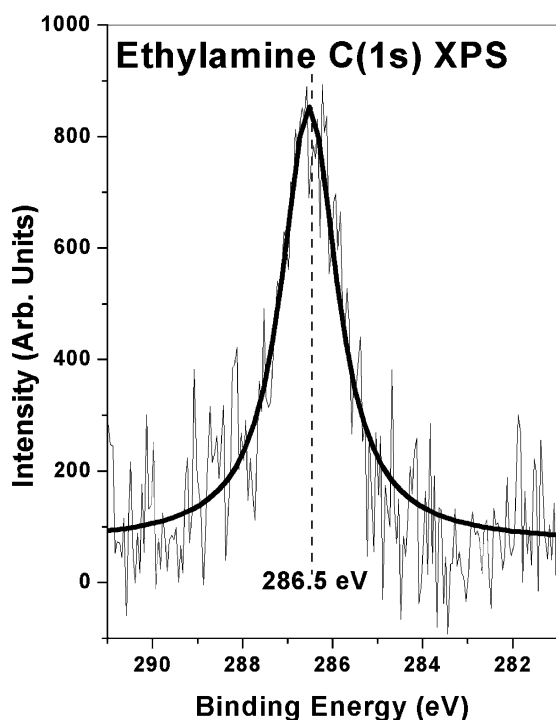
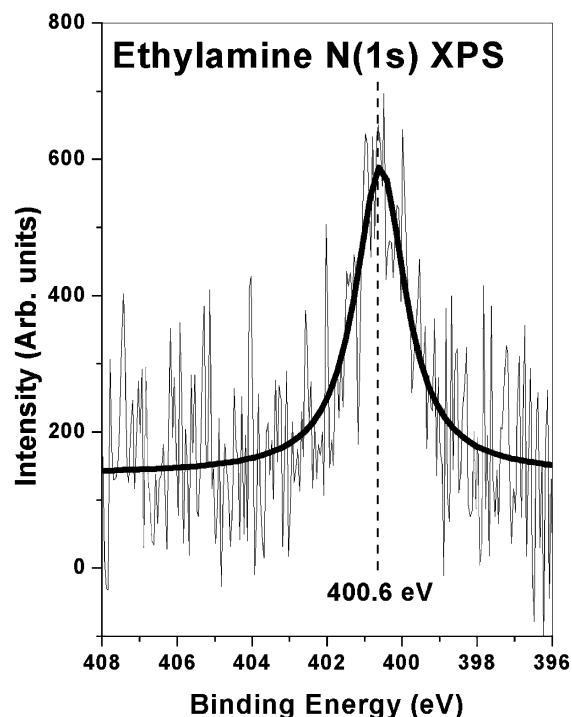


**Figure 9.** Nitrogen 1s XPS spectrum (top) and carbon 1s XPS spectrum (bottom) obtained after a saturation exposure of ethylamine onto the stoichiometric  $\text{TiO}_2(110)$  surface taken at room temperature.

eV and had a fwhm of 1.63 eV, supporting the claim that ethylamine adsorbs intact on this surface. The binding energy observed was similar to that observed for ammonia and dimethylamine, suggesting that ethylamine also binds through the nitrogen atom to the  $\text{Ti}^{4+}$  cations on the surface. Again, it was expected that the two TPD peaks would correspond to two different XPS features indicating two different binding configurations for the nitrogen in ethylamine, but that was not the case. The C(1s) XPS spectrum observed after ethylamine adsorption at room temperature on the stoichiometric surface

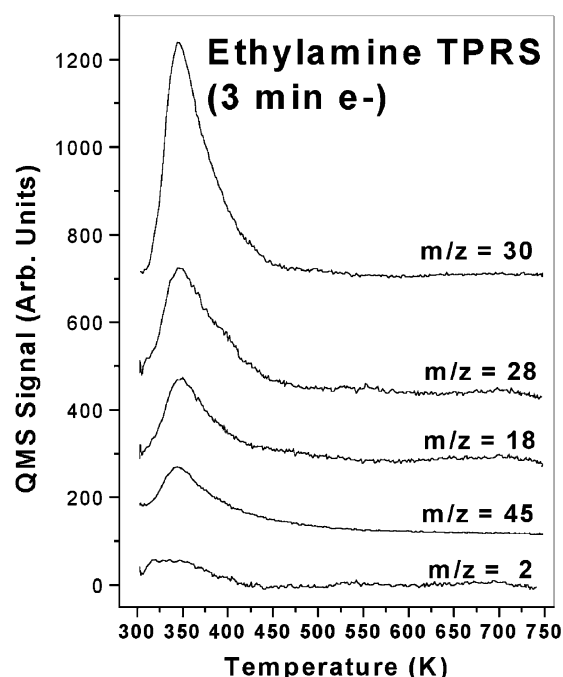


**Figure 10.** TPRS spectrum after ethylamine adsorption onto a  $\text{TiO}_2(110)$  surface that had been preexposed to electron bombardment for 3 min.

is shown in Figure 9. Only one peak was observed, centered at 286.5 eV with a fwhm of 1.51 eV. Although ethylamine has two different carbon environments, they are similar enough to appear together as one peak in the XPS spectrum. The similar structures and binding energies observed for ethylamine and ethanol,<sup>33</sup> in addition to the fact that ethanol was shown to adsorb on the  $\text{Ti}^{4+}$  through its oxygen atom, lead us to propose that ethylamine adsorbed onto the  $\text{Ti}^{4+}$  cations through its nitrogen atom in the same manner.

The TPRS spectrum after ethylamine desorption from a surface that had been preexposed to electron bombardment for 3 min is shown in Figure 10. As was the case with dimethylamine, the presence of defects on the surface caused ethylamine to desorb from only one state, as opposed to two on the stoichiometric surface. As in the case of dimethylamine, this result seems to support the idea that the second desorption feature observed on the stoichiometric surface corresponded to ethylamine bound to an oxygen adatom, because exposing the surface to 300 eV electrons would have removed the existing oxygen adatoms,<sup>34</sup> so that the second peak would no longer be present on the defective surface. The only ethylamine desorption peak shifted 3 K to lower temperature, the same trend as shown by dimethylamine and several aliphatic alcohols on this surface.<sup>33,35</sup> The amount of decomposition products observed was smaller than that produced on the stoichiometric surface but not to a significant extent. This behavior was the same as for dimethylamine but contrary to that observed for alcohols, suggesting that defects do not play a role in the decomposition of amines. Integration of the areas under the TPD peaks showed that the amount of ethylamine desorbed from the defective surface was  $\sim 3\%$  lower than that desorbed from the stoichiometric surface. This decrease in coverage in the presence of defects was also observed for ammonia and dimethylamine, suggesting that adsorption on a point defect (oxygen vacancy) blocks adsorption on more than one neighboring  $\text{Ti}^{4+}$  site, as Siu et al. had proposed for the case of ammonia.<sup>1</sup> The small difference in coverage observed between stoichiometric and

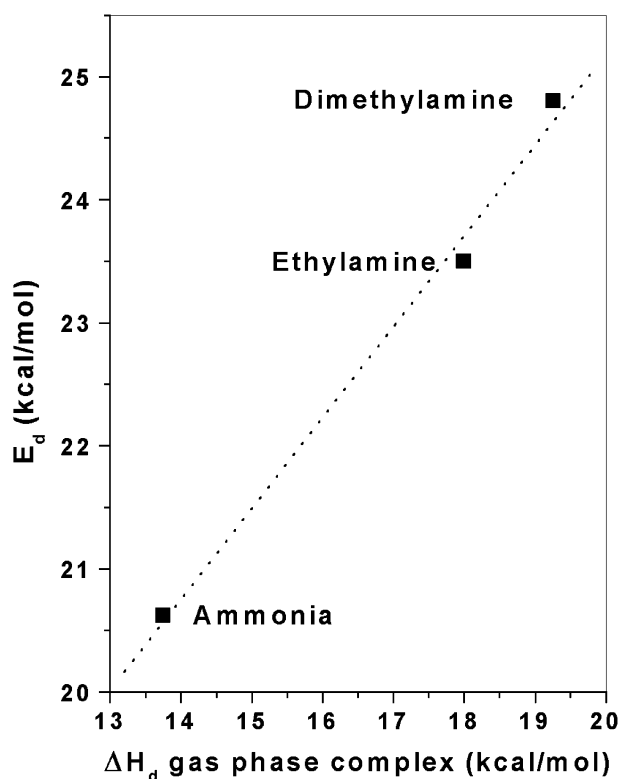


**Figure 11.** Activation energies for desorption of the amines from the stoichiometric  $\text{TiO}_2(110)$  surface vs the heats of dissociation of the respective gas-phase trimethylboron-amine complexes.

defective surfaces for ethylamine suggests that the more bulky ethylamine molecules are exhibiting a blocking effect when bound to  $\text{Ti}^{4+}$  cations as well as when bound to vacancies. An ethylamine molecule bound on a  $\text{Ti}^{4+}$  site could block access to  $\text{Ti}^{4+}$  sites in a similar proportion as an ethylamine molecule bound on a vacancy. The creation of defects on the surface would result in more ethylamine molecules being bound on vacancies, but would not then add significantly to the blocking effect, resulting in a smaller reduction in coverage than observed for ammonia.

**Acidity of  $\text{Ti}^{4+}$  Cations.** The results previously reported in this work suggest that ammonia, dimethylamine, and ethylamine are bound through their nitrogen end groups to the  $\text{Ti}^{4+}$  cations on the stoichiometric  $\text{TiO}_2(110)$  surface. The activation energies for desorption of the amines were determined from the respective TPD curves using the treatment developed by Redhead.<sup>37</sup> Assuming a value of  $10^{13} \text{ s}^{-1}$  for the preexponential factor, the activation energies for desorption of ammonia, dimethylamine, and ethylamine were determined to be 20.6, 24.8, and 23.5 kcal/mol, respectively. If there were a Lewis acid-base type interaction between the adsorbates and the surface, the respective desorption temperatures of the adsorbates should reflect the gas-phase basicity scale of the probe molecules. This was indeed the case. According to gas-phase Lewis basicity data reported in the literature, the probe molecules can be listed in order of decreasing basicity as dimethylamine > ethylamine > ammonia.<sup>38,39</sup> This ordering is not surprising given the electron-donating character of the methyl groups, which facilitate electron sharing by the nitrogen atom in the substituted amines. The relationship between surface acidity and gas-phase acidity is shown in Figure 11. The activation energies for desorption of the amines reported in this work also follow the order dimethylamine > ethylamine > ammonia, suggesting that the

interaction between the surface  $\text{Ti}^{4+}$  cations and the amines is of Lewis acid-base character.

## Conclusion

Ammonia, dimethylamine, and ethylamine were adsorbed mainly intact on stoichiometric and electron-bombarded  $\text{TiO}_2(110)$  surfaces. On the stoichiometric surface, adsorption occurs through the formation of a N-Ti bond with the surface  $\text{Ti}^{4+}$  cations. On the defective surfaces, adsorption occurs on the vacancies as well as the cations, with no additional decomposition products observed. The coverage on the defective surfaces was shown to decrease from that on the stoichiometric surface, suggesting that adsorption on the point defects blocks adsorption at more than one neighboring  $\text{Ti}^{4+}$  cation. The gas-phase basicity scale of the amines was shown to correlate with the desorption temperatures of the species from the surface, reflecting the Lewis acid character of the  $\text{Ti}^{4+}$  cations.

**Acknowledgment.** The authors gratefully acknowledge the support of the National Science Foundation through NSF Grant CTS 0000283.

## References and Notes

- (1) Siu, W. K.; Bartynski, R. A.; Hulbert, S. L. *J. Chem. Phys.* **2000**, *113*, 10697.
- (2) Román, E. L.; de Segovia, J. L.; Kurtz, R. L.; Stockbauer, R.; Madey, T. E. *Surf. Sci.* **1992**, *273*, 40.
- (3) Diebold, U.; Madey, T. E. *J. Vac. Sci. Technol. A* **1992**, *10*, 2327.
- (4) Román, E. L.; de Segovia, J. L. *Surf. Sci.* **1991**, *251*, 742.
- (5) Boddenberg, B.; Eltzner, K. *Langmuir* **1991**, *7*, 1498.
- (6) Epling, W. S.; Peden, C. H. F.; Henderson, M. A.; Diebold, U. *Surf. Sci.* **1998**, *412*, 333.
- (7) Kim, K. S.; Barteau, M. A.; Farneth, W. E. *Langmuir* **1988**, *4*, 533.
- (8) Göpel, W.; Anderson, J. A.; Frankel, D.; Jaehnig, M.; Phillips, K.; Schäfer, J. A.; Rucker, G. *Surf. Sci.* **1984**, *139*, 333.
- (9) Hugenschmidt, M. B.; Gamble, L.; Campbell, C. T. *Surf. Sci.* **1994**, *302*, 329.
- (10) Pétingy, S.; Mostéfa-Sba, H.; Domenichini, A.; Lenieswska, E.; Steinbrunn, A.; Bourgeois, S. *Surf. Sci.* **1998**, *410*, 250.
- (11) Göpel, W.; Rucker, G.; Feierabend, R. *Phys. Rev. B* **1983**, *28*, 3427.
- (12) Onishi, H.; Iwasawa, Y. *Surf. Sci.* **1994**, *313*, L783.
- (13) Cocks, I. D.; Guo, Q.; Williams, E. M. *Surf. Sci.* **1997**, *390*, 119.
- (14) Wang, L.; Baer, D. R.; Engelhard, M. H. *Surf. Sci.* **1994**, *320*, 295.
- (15) Pan, J. M.; Maschhoff, B. L.; Diebold, U.; Madey, T. E. *J. Vac. Sci. Technol. A* **1992**, *10*, 2470.
- (16) Wang, L.; Schultz, A. N.; Baer, D. R.; Engelhard, M. H. *J. Vac. Sci. Technol. A* **1996**, *14*, 1532.
- (17) Rucker, G.; Göpel, W. *Surf. Sci.* **1986**, *175*, L675.
- (18) Linsebigler, A.; Lu, G.; Yates, J. T., Jr. *J. Chem. Phys.* **1995**, *103*, 9438.
- (19) Lo, W. J.; Chung, Y. W.; Somorjai, G. A. *Surf. Sci.* **1978**, *71*, 199.
- (20) Tanabe, K. In *Catalysis Science and Technology*; Anderson, J. R., Boudart, M., Eds.; Springer-Verlag: Berlin, 1980; Vol. 2, p 232.
- (21) *New Solid Acids and Bases*; Tanabe, K.; Misono, M.; Ono, Y., Hattori, H., Eds.; Kodansha, Ltd., and Elsevier Science Publishers B.V.: Tokyo, 1989; Vol. 51.
- (22) Moffat, J. B. The Acidity and Basicity of Solids: Intrinsic Properties of the Surface, Its Structure and Composition. In *Acidity and Basicity of Solids. Theory, Assessment and Utility*; Fraissard, J., Petakis, L., Eds.; Kluwer Academic Publishers: Dordrecht, The Netherlands, 1994; Vol. 444.
- (23) Barteau, M. A.; Madix, R. J. *Surf. Sci.* **1982**, *120*, 262.
- (24) Spitz, R. N.; Barton, J. E.; Barteau, M. A.; Staley, R. H.; Sleight, A. W. *J. Phys. Chem.* **1986**, *90*, 4067.
- (25) Suzuki, S.; Yamaguchi, Y.; Onishi, H.; Sasaki, T.; Fukui, K.; Iwasawa, Y. *J. Chem. Soc., Faraday Trans.* **1998**, *94*, 161.
- (26) Suzuki, S.; Onishi, H.; Fukui, K.; Iwasawa, Y. *Chem. Phys. Lett.* **1999**, *304*, 225.
- (27) Suzuki, S.; Yamaguchi, Y.; Onishi, H.; Fukui, K.; Sasaki, T.; Iwasawa, Y. *Catal. Lett.* **1998**, *50*, 117.
- (28) Wang, Q. Ph.D. Thesis, Stanford University, Stanford, CA, 2001.
- (29) Eriksen, S.; Egdell, R. G. *Surf. Sci.* **1987**, *180*, 263.
- (30) Wang, L. Q.; Ferris, K. F.; Shultz, A. N.; Baer, D. R.; Engelhard, M. H. *Surf. Sci.* **1997**, *380*, 352.
- (31) Sambì, M.; Sangiovanni, G.; Grazzozzi, G.; Parmigiani, F. *Phys. Rev. B* **1997**, *55*, 7850.



- (32) Farfan-Arribas, E.; Madix, R. J., manuscript to be submitted.
- (33) Farfan-Arribas, E.; Madix, R. J. *J. Phys. Chem. B* **2002**, 106, 10680.
- (34) Iwasawa, Y.; Onishi, H.; Fukui, K. *Top. Catal.* **2001**, 14, 163.
- (35) Gamble, L.; Jung, L. S.; Campbell, C. T. *Surf. Sci.* **1996**, 348, 1.
- (36) Henderson, M. A. *Langmuir* **1996**, 12, 5093.
- (37) Redhead, P. A. *Vacuum* **1962**, 12, 203.
- (38) Brown, H. C.; Bartholomay, H. J.; Taylor, M. D. *J. Am. Chem. Soc.* **1944**, 66, 435.
- (39) Brown, H. C.; Taylor, M. D.; Sujishi, S. *J. Am. Chem. Soc.* **1951**, 73, 2464.